frontiers | Frontiers in Materials

TYPE Original Research
PUBLISHED 19 September 2023
DOI 10.3389/fmats.2023.1273659

OPEN ACCESS

EDITED BY
Zequn Cui,
Nanyang Technological University, Singapore

REVIEWED BY
Yichao Wang,
Western Sydney University, Australia
Xiang Qi,
Xiangtan University, China

*CORRESPONDENCE
Bao Lin,
linbao@hdu.edu.cn
Xiaolan Wei,
weixiaolan@proya.com

RECEIVED 07 August 2023
ACCEPTED 08 September 2023
PUBLISHED 19 September 2023

CITATION
Yang P, Wang H, Chen Y, Li Y, Zhang J, Zhang C, Lin B and Wei X (2023), Ball-milling of titanium dioxide and zinc oxide for enhanced UV protection. *Front. Mater.* 10:1273659. doi: 10.3389/fmats.2023.1273659

Ball-milling of titanium dioxide and zinc oxide for enhanced UV protection

Panpan Yang[1], Hongxia Wang[1], Yuyan Chen[1], Yanan Li[1], Jun Zhang[2], Chunxiao Zhang[2], Bao Lin[2]* and Xiaolan Wei[1]*

[1]Proya Cosmetics Co., Ltd., Hangzhou, China, [2]College of Materials and Environmental Engineering, Hangzhou Dianzi University, Hangzhou, China

Among various sunscreen materials, zinc oxide and titanium dioxide are excellent physical sunscreen components; however, these two materials tend to aggregate and form micrometer-sized particles that may impact their performance. This study utilizes fine grinding techniques to break up the aggregated oxide particles into small nanoparticles with a narrow size distribution averaging around 200 nm in diameter. The ground zinc oxide and titanium dioxide particles exhibit enhanced ability in absorbing and scattering ultraviolet radiation compared to their original state before grinding. Consequently, this research offers innovative concepts as well as approaches towards developing highly efficient yet low-toxic physical sunscreen components while significantly contributing to the preparation process optimization for mixed material performance.

KEYWORDS

ball milling, sunscreen, free radicals, UV absorption, SPF

1 Introduction

In recent years, due to escalating pollution and ozone layer depletion, solar radiation has increasingly become detrimental to human skin (Sakamoto et al., 1995; Armstrong and Kricker, 2001; Bo-Wen et al., 2017; Xinrui et al., 2018). Ultraviolet (UV) radiation is a crucial constituent of sunlight and can be categorized into three wavelength bands: UVA, UVB, and UVC (Burnett and Wang, 2011). Among these, UVA and UVB are the primary wavelengths responsible for human skin damage. Consequently, an increasing number of individuals are focusing on effective strategies to safeguard their skin against these harmful rays. More and more people concern to how to effectively shield themselves from ultraviolet rays. Sunscreen, as a daily sun care product, can effectively block or absorb UV rays, thus achieving the protective effect on human skin (Burnett and Wang, 2011; Smijs and Pavel, 2011). Currently, titanium dioxide (TiO_2) and zinc oxide (ZnO) are commonly used as the primary sunscreen ingredients in physical daily sunscreen products. TiO_2 exhibits an absorption peak near 290 nm, providing predominantly UVB protection, while ZnO has an absorption peak at 360 nm that falls between UVB and UVA wavelengths, making it an excellent component for creating a comprehensive spectral sunscreen agent when combined with TiO_2 (Smijs and Pavel, 2011; Reinosa et al., 2016). These substances primarily mitigate the impact of ultraviolet radiation on human skin through scattering or reflection mechanisms. Furthermore, when TiO_2 and ZnO are used together as composite materials in sunscreens, TiO_2 and ZnO forms a denser composite structure that enhances both UV protection performance and photostability (Reinosa et al., 2016).

Previous studies have demonstrated that the particle morphology of physical sunscreens influences their UV absorption rates (Lee et al., 2023). Different particle sizes can also impact free radical production and viscosity (Salah et al., 2011). It is widely accepted that decreasing particle size enhances UV absorption efficiency while increasing free radical production (Ishibashi et al., 2000; Salah et al., 2011), particularly when the size approaches the wavelength of UV light, leading to scattering in all directions and reducing its intensity (Murphy, 1999). However, since free radicals accelerate skin aging and sunscreen degradation (Konaka et al., 1999; Konaka et al., 2001; Mirhosseini and Firouzabadi, 2013; Wang et al., 2022a), antioxidants must be incorporated to counteract these effects during practical application. Moreover, due to potential toxicity associated with nanomaterials (Epstein, 2011; Baek et al., 2017), a meticulous approach is necessary for utilizing nanomaterials. Therefore, a balance needs to be achieved between particle size and sunscreen effectiveness in applications.

In this study, a slurry of zinc oxide and titanium dioxide was prepared, and the particle size of both metallic oxides was reduced through ball milling before being used in sunscreen. The impact of slurry particle size on the morphology, generation of free radicals, viscosity, application uniformity, and SPF index of sunscreen samples was investigated.

2 Materials and methods

2.1 Preparation of materials

The pristine ZnO and TiO_2 particles were commercial products supplied by Proya Cosmetics Co., Ltd. They were mixed together to form a raw slurry. The slurry was then milled in steel cells (200 mL) using zirconia balls (Φ200 μm) in an air environment. The milling process was performed continuously two times, with durations of 3 and 2 min respectively. Mechanical milling took place in a horizontal oscillatory mill (Retsch, PM 400) operating at 3,000 rpm. The volume ratio of zirconia balls to slurry was approximately 2:1. Two parallel cells were used for this experiment, with the total weight of the slurry being 70 g. After milling, the milling media was filtered out and the resulting slurry was made into sunscreen cream by Proya Cosmetics Co., Ltd., followed by subsequent analysis.

2.2 Characterisation

The morphology of the Slurry was characterized using a field emission scanning electron microscope (FESEM), APREO-S, (FEI, United States) operated at 10 kV. Particle size analysis was conducted with a laser diffraction analyzer BT-2001 (Bettersize, China). The Slurry was diluted with ethanol to achieve a dilution factor of 20,000 and then slowly transferred to the sampling cell for determination of particle size distribution in triplicate.

2.3 UV-VIS absorbance

The effect of milling was tested by applying 2 mg·cm^{-2} of the Slurry and correlated Cream on three quartz glass sheets measuring 40 mm * 40 mm * 1 mm. Three transmission measures were performed on each plate in a wavelength range of 200–600 nm using a spectrophotometer UV-3600 (Shimadzu, Japan). To ensure correct application density, the plates were weighed before and after product application. The samples were allowed to settle for 15 min in the dark at room temperature to ensure self-leveling of the formulation.

2.4 Viscosity test

The viscosity test of the Cream in this experiment was conducted using a Brookfield viscometer DV-II (Brookfield, United States) with the 2nd rotor selected for testing lower viscosity and adjusted to 6 rpm. Data recording was performed when the readings stabilized, and the measurement progress on the right side ascended from bottom to top.

2.5 Free radical test

The active species of the photocatalysts were confirmed by detecting hydroxyl radicals (OH•) at the photo-illuminated interface between the photocatalyst and water using fluorescence (FL) technique with terephthalic acid as a probe molecule (Ishibashi et al., 2000). Terephthalic acid reacts with OH• to produce a highly fluorescent product, 2-hydroxyterephthalic acid. In this experiment, a uniform cream was applied onto a 1 cm * 1 cm glass slide, which was then placed at the bottom of a glass square container with matching dimensions. A solution containing 3×10^{-3} M terephthalic acid and NaOH at a concentration of 1×10^{-2} M was added into the container (100 mL). Irradiation was performed using a xenon lamp with an output power of 300 W. Every 10 min, a sample volume of 3 mL was extracted to assess OH• generation by measuring changes in FL intensity emitted from 2-hydroxyterephthalic acid excited by light at wavelength of 325 nm on a fluorescence spectrophotometer (RF-539TPC, Shimadzu, Japan).

2.6 Skin surface profilometry

The skin surface structure was measured using a noncontact 3D-profilometer (Bruker ContourGT-X, Germany). In this study, the 3D-profilometer was used to assess the surface roughness after sunscreen application since a higher film forming capacity leads to better reduction of surface roughness. For this test, small pieces (2 cm * 1 cm) of pig facial skin cut from a big pig facial skin were prepared. Each sample was uniformly applied on the pig skin following a rule of 2 mg·cm^{-2}. Random areas (1 mm * 1 mm) were scanned using the 3D-profilometer. The scanned results obtained were processed and analyzed using Vision64 software (Bruker, Germany).

2.7 SPF *in vivo*

The study adhered to the *Safety and Technical Standards for Cosmetics* (2022) and was carried out in accordance with the ethical

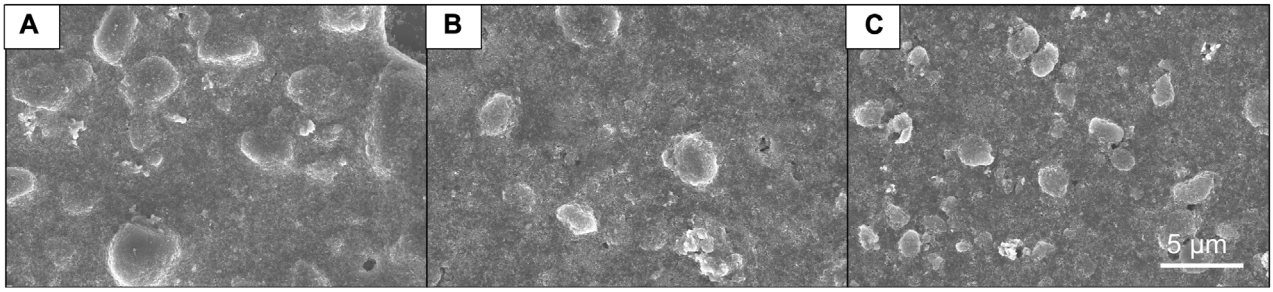

FIGURE 1
SEM image of Slurry. **(A)** WM, **(B)** MO, **(C)** MT.

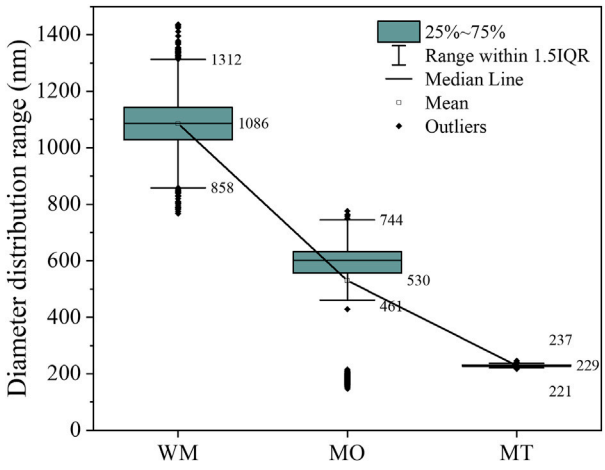

FIGURE 2
The particle size analysis conducted by the laser particle analyzer on the Slurry diluted 20,000 times.

standards of the Declaration of Helsinki of 1975, as revised in 2013. All the participants provided their consent before the start of this study. Proya Cosmetics Co., Ltd., in Hangzhou, Zhejiang Province, China, performed the *in vivo* SPF measurements.

3 Results

3.1 Characterization and test on the slurry

The SEM analysis was performed on a mixed slurry of TiO2 and ZnO, and the resulting images are presented in Figure 1. Figures 1A–C correspond to the Slurry without milling (WM), the Slurry with one round of milling (MO), and the Slurry with two rounds of milling (MT), respectively. The metallic oxide particles within the field of vision exhibit lustrous edges. Both metallic oxides have a measured size fluctuating between 4 and 6 μm, indicating their tendency to aggregate. After two rounds of milling, particle size reduction was observed to approximately 1 μm.

The data obtained from the laser particle size analyzer, as presented in Figure 2, clearly demonstrates that ball milling effectively reduces the particle size. This is evidenced by a significant decrease in the average value from 1,086 to 229 nm. Simultaneously, there is a remarkable reduction in the standard deviation from 460.36 to 2.97 nm, indicating enhanced uniformity of metallic oxide particles through ball milling.

The Figure 3A illustrates the comparison of UV-VIS transmission absorption spectra data for the Slurry before and after ball-milling. The absorption spectra indicate a decrease in the rate of light absorption, particularly in the visible light range (>390 nm), with an increasing number of ball milling cycles. In contrast, in the ultraviolet range (<360 nm), regardless of whether it is subjected to ball-milling or not, the absorption rate remains close to 100% without any significant difference ($p > 0.05$).

3.2 Test on the sunscreen creams made from correlated milled Slurries

The Sunscreen cream (Cream) was formulated using both milled and pristine Slurry as raw materials. The Figure 3B illustrates the comparison of UV-VIS transmission absorption spectra data for the Cream. In comparison to the Slurry, the Cream samples exhibit significantly lower absorption rates across the entire spectrum, which absorption rate of visible light is less than 50%. For sunscreens requiring effective UV protection, Cream samples demonstrate absorption rates ranging from 66% to 83% in the UV range. A non-parametric sign test conducted on different Cream samples' absorption rate data revealed that the UV-VIS transmittance rates of Cream samples were as follows: MT > MO > WM ($p < 0.01$).

The viscosity of the Cream was measured, revealing a significant increase in viscosity from 148 to 4,900 CPS with each successive milling process applied to the Slurry, as presented in Table 1. Even a single milling process resulted in the Cream viscosity of 3,700, which is an order of magnitude higher than that of WM.

The skin surface roughness was evaluated using pig skin *ex vivo* through 3D-profilometry, 30 min after the application of sunscreen, as shown in Table 2. An ascending order of roughness data (MT > MO > WM) was observed as the number of milling increased ($p < 0.01$). The untreated pig skin exhibits a slightly higher roughness compared to the pig skin coated with WM, but it is lower than that of the pig skin coated with MO and MT samples.

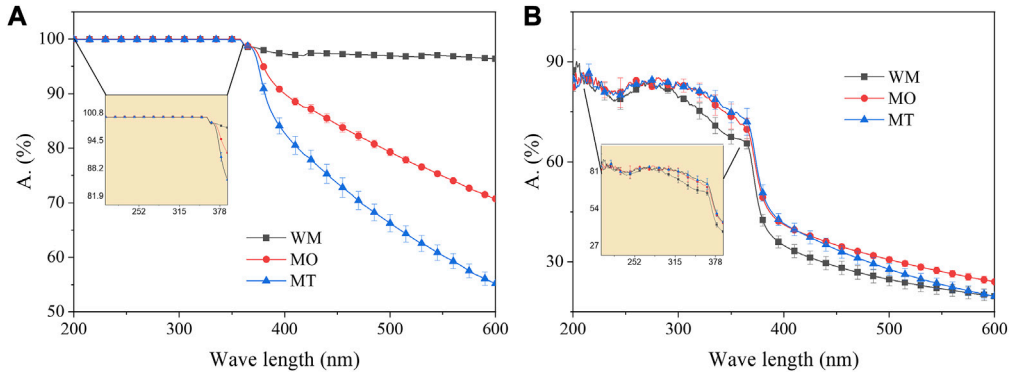

FIGURE 3
The UV-VIS absorption spectrum. **(A)** The Slurry. **(B)** The Cream.

TABLE 1 The viscosity of Creams made of correlated milled Slurries.

	Viscosity (CPS)
WM	148
MO	3,700
MT	4,900

The Figure 4 shows the fluorescence (FL) effects of the Cream made from milled Slurries. The Table 3 demonstrates that the slope of FL intensity over time represents the production of free radicals in the Cream. From the results, it can be observed that the production of free radicals in the Cream made from MT samples is significantly lower than that of WM and MO, accounting for only about 13% of WM, which is 6.34 ± 0.96 (a.u.·h^{-1}).

The SPF values of the Creams, as presented in Table 4, are 31.34 ± 3.0, 35.24 ± 0.4, and 44.86 ± 5.2 respectively. The differences in SPF, among the Creams were found to be highly significant ($p < 0.01$).

4 Discussion

Ball milling is a top-down processing technique in which larger particles of raw materials are transformed into smaller particles. When employing ball milling for the production of sub-micron level powders, its distinctive features, compared to bottom-up synthesis techniques, are exhibited in the homogeneous composition of the final product and a narrower range of particle size distribution since the milling media continuously crushes the sample until it reaches a critical size. Therefore, the disparity between SEM photos and laser particle size analyzer data can be attributed to particle aggregation phenomena. Although ball milling can disperse aggregated particles to some extent, complete prevention of aggregation remains challenging due to the absence of dispersants. Nevertheless, considering concerns regarding nanomaterial toxicity (Spisni et al., 2016) an alternative approach could involve increasing the volume of nano-oxide particles obtained through aggregation during ball milling within safe limits.

It is widely accepted that the smaller the nanoparticle, the higher its ultraviolet light absorption capacity (Surber et al., 2021). The results of this experiment, however, revealed a trend in visible light absorption: WM > MO > MT. This suggests that as the particle size decreases, there is a decrease in the efficiency of visible light absorption. This phenomenon may be attributed to a decrease in scattering efficiency for longer wavelengths of visible light upon reducing the size of metallic oxide particles. In contrast, there was no statistically significant difference ($p > 0.05$) in ultraviolet light absorption rates. It is speculated that the Slurry with a thickness of 2 mg·cm^{-2} was excessively thick and completely absorbed ultraviolet light. It is important to note that in sunscreens, a decrease in absorption of visible light is advantageous rather than disadvantageous. This leads to enhanced transparency upon application to the skin, allowing for a natural appearance without concerns about whitening. During the formulation process of sunscreen cream from the Slurry, it has been observed that the light absorption efficiency of the Cream is inversely proportional to that of the

TABLE 2 Skin surface roughness obtained *ex vivo* for each Cream sample.

	Pig skin	WM	MO	MT
Sa[a]	13.31 ± 2.71	12.55 ± 1.78	18.37 ± 0.77	19.63 ± 1.73
Sq[a]	16.63 ± 3.14	15.8 ± 1.75	22.8 ± 1.47	25.39 ± 2.64
Ssk[a]	0.31 ± 0.27	−0.08 ± 0.39	−0.11 ± 0.14	−0.27 ± 0.37
Sku[a]	3.02 ± 0.25	3.21 ± 0.67	2.88 ± 0.23	3.86 ± 0.25
Sz[a]	136.03 ± 21.15	115.41 ± 11.32	181.57 ± 28.03	221.29 ± 33.39

[a]Sa, mean roughness; Sq, root mean square roughness; Ssk, skewness of the 3D surface texture; Sku, Kurtosis of the 3D surface texture; Sz is the Ten Point Height over the complete 3D surface.

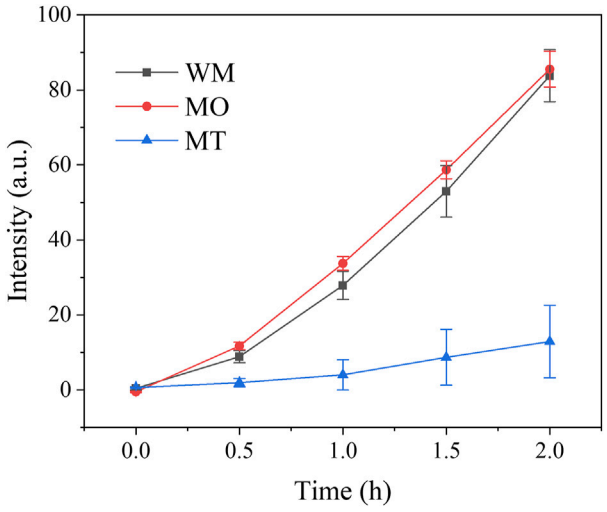

FIGURE 4
The FL intensity of Creams, made from correlated milled Slurries, exhibits time-dependent changes at 425 nm in a xylene solution upon exposure to 325 nm light.

TABLE 3 Free radical production of Creams made from correlated milled Slurries.

	K^a (a.u.·h^{-1})
WM	46.61 ± 3.62
MO	47.31 ± 1.46
MT	6.34 ± 0.96

[a]K represents the rate of change in FL intensity over time.

TABLE 4 SPF of Creams made of correlated milled Slurries.

Seq	WM	MO	MT
1	33.0	35.0	51.6
2	29.6	35.0	44.9
3	34.0	36.0	44.9
4	29.6	35.0	39.0
5	26.5	35.0	39
Average	30.5	35.2	43.9
Standard deviation	3.0	0.4	5.2
Variability	—	4.7	13.3
Rate of change	—	15.3%	43.7%
p-value vs. without milling	—	0.0092	0.0011
	—	**	**
p-value vs. milling once	—	—	0.0061
	—	—	**

**$0.001 \leq p < 0.01$.

correlated Slurry, with MT > MO > WM. By analyzing the data obtained from the Slurry (Figure 3A), it can be inferred that this decrease in light absorption may be attributed to a relative reduction in ZnO and TiO_2 content caused by the addition of other ingredients during the formulation process of the Cream. Therefore, milled slurry exhibits a lesser decrease in its absorption rate as the content decreases. It implies that ball milling treatment can effectively reduce ZnO and TiO_2 dosage of the Cream.

The viscosity sunscreen cream made from correlated milled Slurry increased significantly by an order of magnitude, rising from 148 CPS to over 20 times higher at 3,700 CPS, and second ball milling further elevated the viscosity of correlated Cream to 4,900 CPS. This phenomenon can be attributed to a reduction in particle size and an increase in specific surface area, thereby enhancing interactions with other organic components present in the sunscreen formulation. The roughness of pig skin coated with MO and MT, which exhibit higher viscosity, is greater than that of WM and even the uncoated pig skin. Increasing viscosity does not impact the film-forming capacity of sunscreen cream; however, it significantly affects the ability of sunscreen cream to fill in skin surface grooves.

It is worth noting that the free radical production of Cream made from MT is significantly lower compared to that of WM and MO, accounting for approximately 13% of WM. For the sunscreens, free radicals play a negative role as they have the potential to damage skin cells. Therefore, commercial products often incorporate antioxidants such as vitamin C, vitamin E, or tea polyphenols, and etc. It is widely accepted that the smaller particle size leads to the higher free radical production (Salah et al., 2011; Wang et al., 2022b); the contradictory result in this work may be attributed to enhanced contact between small particles and antioxidants. Simultaneously, the Cream made from correlated milled Slurry exhibits a significantly increased Sun Protection Factor (SPF) when compared to WM ($p > 0.01$). Considering that SPF relies not only on material UV absorption but also on scattering and diffuse reflection factors. Therefore, ball milling was undoubtedly a viable method for enhancing sunscreens by reducing the particle size of metallic oxides.

5 Conclusion

A submicron slurry containing TiO_2 and ZnO powders with particle size of 229 ± 2.9 nm measured by laser particle analyser was produced by utilizing pre-mixed TiO_2 and ZnO powders after two rounds of ball milling. In comparison to the pristine slurry without milling, the sunscreen cream formulated from the milled slurry exhibited a dramatic 87% reduction in free radical generation, measuring only 6.34 ± 0.96 a.u.·h^{-1}; and its viscosity presented a substantial increase by 30 times, reaching 4,900 CPS; simultaneously, the SPF value has significantly improved by 43%, resulting in an impressive measurement of 44.86 ± 5.2. It can be concluded that this method of ball milling effectively enhances the performance of sunscreen products.

Data availability statement

The raw data supporting the conclusion of this article will be made available by the authors, without undue reservation.

Ethics statement

The studies involving humans were approved by the Ethics committee, Proya Cosmetics Co., Ltd. The studies were conducted in accordance with the local legislation and institutional requirements. Written informed consent for participation in this study was provided by the participants' legal guardians/next of kin.

Author contributions

PY: Formal Analysis, Investigation, Resources, Writing–review and editing. HW: Formal Analysis, Investigation, Writing–review and editing. YC: Formal Analysis, Investigation, Writing–review and editing. YL: Writing–review and editing. JZ: Formal Analysis, Methodology, Supervision, Writing–review and editing. CZ: Data curation, Investigation, Resources, Writing–review and editing. BL: Formal Analysis, Methodology, Writing–original draft. XW: Funding acquisition, Project administration, Supervision, Writing–review and editing.

Funding

The author(s) declare that no financial support was received for the research, authorship, and/or publication of this article.

Acknowledgments

The authors would like to express their gratitude to Mr. Yang Shuai and Miss Lin Jiachen for their invaluable support and assistance throughout the experimental phase of this research.

Conflict of interest

Authors PY, HW, YC, YL, and XW were employed by Proya Cosmetics Co., Ltd.

The remaining authors declare that the research was conducted in the absence of any commercial or financial relationships that could be construed as a potential conflict of interest.

Publisher's note

References

Armstrong, B. K., and Kricker, A. (2001). The epidemiology of UV induced skin cancer. *J. Photochem Photobiol. B* 63 (1–3), 8–18. doi:10.1016/s1011-1344(01)00198-1

Baek, S., Joo, S. H., Kumar, N., and Toborek, M. (2017). Antibacterial effect and toxicity pathways of industrial and sunscreen ZnO nanoparticles on Escherichia coli. *J. Environ. Chem. Eng.* 5 (3), 3024–3032. doi:10.1016/j.jece.2017.06.009

Bo-Wen, L. I., Qing, H., Ying-Jie, D., Shi-Kang, T., Xian, W. U., Li-Hua, L. I., et al. (2017). Research and application progress of nano UV-shielding materials. *Contemp. Chem. Ind.* doi:10.3969/j.issn.1671-0460.2017.12.055

Burnett, M. E., and Wang, S. Q. (2011). Current sunscreen controversies: A critical review. *Photodermatol. Photoimmunol. Photomed.* 27 (2), 58–67. doi:10.1111/j.1600-0781.2011.00557.x

Epstein, H. A. (2011). Nanotechnology in cosmetic products. *Skinmed* 9 (2), 109–110.

Ishibashi, K., Ishibashi, K., Fujishima, A., Fujishima, Akira, Watanabe, T., and Hashimoto, K. (2000). Detection of active oxidative species in TiO2 photocatalysis using the fluorescence technique. *Electrochem. Commun.* 2 (3), 207–210. doi:10.1016/s1388-2481(00)00006-0

Konaka, R., Kasahara, E., Dunlap, W. C., Yamamoto, Y., Chien, K. C., and Inoue, M. (1999). Irradiation of titanium dioxide generates both singlet oxygen and superoxide anion. *Free Radic. Biol. Med.* 27 (3–4), 294–300. doi:10.1016/S0891-5849(99)00050-7

Konaka, R., Kasahara, E., Dunlap, W. C., Yamamoto, Y., Chien, K. C., and Inoue, M. (2001). Ultraviolet irradiation of titanium dioxide in aqueous dispersion generates singlet oxygen. *Redox Rep.* 6 (5), 319–325. doi:10.1179/135100001101536463

Lee, J.-H., Lee, G.-S., Park, E.-N., Jo, D.-H., Kim, S.-W., and Lee, H.-C. (2023). Synthesis of planar-type ZnO powder in non-nano scale dimension and its application in ultraviolet protection Cosmetics. *Materials* 16 (5), 2099. doi:10.3390/ma16052099

Mirhosseini, M., and Firouzabadi, F. B. (2013). Antibacterial activity of zinc oxide nanoparticle suspensions on food-borne pathogens. *Int. J. Dairy Technol.* 66 (2), 291–295. doi:10.1111/1471-0307.12015

Murphy, G. M. S. (1999). Sunblocks: mechanisms of action. *Photodermatol. Photoimmunol. Photomed.* 15 (1), 34–36. doi:10.1111/j.1600-0781.1999.tb00051.x

Reinosa, J. J., Leret, P., Álvarez-Docio, C. M., del Campo, A., and Fernández, J. F. (2016). Enhancement of UV absorption behavior in ZnO–TiO2 composites. *Bol. Soc. española cerámica Vidr.* 55 (2), 55–62. doi:10.1016/j.bsecv.2016.01.004

Sakamoto, M., Okuda, H., Futamata, H., Sakai, A., and Iida, M. (1995). Influence of particle size of titanium dioxide on UV-ray shielding property. *J. Jpn. Soc. Colour Material* 68, 203–210. doi:10.4011/shikizai1937.68.203

Salah, N., Habib, S. S., Khan, Z. H., Memic, A., Azam, A., Al-Hamedi, E., et al. (2011). High-energy ball milling technique for ZnO nanoparticles as antibacterial material. *IJN* 6, 863–869. doi:10.2147/ijn.s18267

Smijs, T. G., and Pavel, S. (2011). Titanium dioxide and zinc oxide nanoparticles in sunscreens: focus on their safety and effectiveness. *Nanotechnol. Sci. Appl.* 4, 95–112. doi:10.2147/nsa.s19419

Spisni, E., Seo, S., Joo, S. H., and Su, C. (2016). Release and toxicity comparison between industrial- and sunscreen-derived nano-ZnO particles. *Int. J. Environ. Sci. Technol. (Tehran)* 13, 2485–2494. doi:10.1007/s13762-016-1077-1

Surber, C., Plautz, J., Dähnhardt-Pfeiffer, S., and Osterwalder, U. (2021). Size matters! Issues and challenges with nanoparticulate UV filters. *Curr. Probl. Dermatol* 55, 203–222. doi:10.1159/000517632

Wang, Y., Zavabeti, A., Haque, F., Zhang, B. Y., Yao, Q., Chen, L., et al. (2022b). Plasmon-induced long-lived hot electrons in degenerately doped molybdenum oxides for visible-light-driven photochemical reactions. *Mater. Today* 55, 21–28. doi:10.1016/j.mattod.2022.04.006

Wang, Y., Zavabeti, A., Yao, Q., Tran, T. L. C., Yang, W., Kong, L., et al. (2022a). Nanobionics-driven synthesis of molybdenum oxide nanosheets with tunable plasmonic resonances in visible light regions. *ACS Appl. Mater. Interfaces* 14 (49), 55285–55294. doi:10.1021/acsami.2c19154

Xinrui, W., Huimin, C., Liping, T., Li, L. I., and Dongpeng, Y. a. N. (2018). Applications of two-dimensional layered nanomaterials in Cosmetics. *Chin. J. Appl. Chem.* 35 (10), 1166. doi:10.11944/j.issn.1000-0518.2018.10.180123